

---

## Control of pulsed gas metal arc welding

---

Jesper Sandberg Thomsen

Department of Control Engineering,  
Institute of Electrical Systems,  
Aalborg University,  
Aalborg, Denmark  
E-mail: jsat@control.aau.dk

**Abstract:** This paper presents a control system for manual pulsed Gas Metal Arc Welding (GMAW). This system consists of a current controller, which makes it possible to shape the current during welding, and two important components, which are the key issues discussed in this paper. These components include an arc length controller and a metal transfer controller. The arc length controller is based on a non-linear SISO model of the arc length process and uses feedback linearisation for cancellation of non-linear terms. The metal transfer controller uses a melting speed model to determine when liquid drops at the tip of the electrode should be detached. Tests are carried out in a simulation environment.

**Keywords:** Gas Metal Arc Welding (GMAW); pulsed welding; control; feedback linearisation; simulation.

**Reference** to this paper should be made as follows: Thomsen, J.S. (2006) 'Control of pulsed gas metal arc welding', *Int. J. Modelling, Identification and Control*, Vol. 1, No. 2, pp.115–125.

**Biographical notes:** Jesper Sandberg Thomsen received an MScEE degree with specialty in Control Engineering in 1998 at Aalborg University, Denmark. In 1998, he was employed as a research assistant in the Department of Control Engineering, Aalborg University and worked on a fault-tolerant control system in a joint project with Mobile Hydraulics Division, Danfoss, Denmark. In 2000, he started as a PhD student in the Department of Control Engineering, Aalborg University and worked on improving control methods for gas metal arc welding. This work was sponsored by the welding machine company Migatronik A/S, Denmark and during the work he spent eight months at the Center for Robotics and Manufacturing Systems, University of Kentucky. In 2004, he received his PhD. Currently, he is an Assistant Professor in the Department of Control Engineering at Aalborg University.

---

### 1 Introduction

Pulsed Gas Metal Arc Welding (GMAW) process is one of several types of welding process, frequently employed in industry. It is performed either as an automated robotic process or as a manual process. In many applications of the pulsed GMAW process high weld quality is of concern, and therefore, it must be considered how such quality is obtained. In GMAW many different aspects contribute to the overall quality of the weld, and one important and significant aspect is the performance of the algorithms controlling the welding process. In this paper, an overall controller for the manual pulsed GMAW process is suggested. This includes two main aspects with respect to control, namely, arc length control and metal transfer control.

Arc length control is used for keeping a steady and stable arc despite disturbances during the welding process, which, for example, could be an uneven movement of the welding gun or irregularities in the workpiece. Arc length control can be performed by a PI-control strategy as

reported by Ozcelik et al. (1998). Another linear control strategy is reported by Zhang et al. (2002), in which robustness is also taken into account. In Abdelrahman (1998), Moore et al. (1999) and Naidu et al. (2003) the GMAW process is considered as a Multi-Input Multi-Output (MIMO) system and non-linearities are cancelled using an additional feedback signal for each controller output. A similar approach is used by Jalili-Kharaajoo et al. (2003), but it uses sliding mode control for the purpose of robustness. However, in most welding machines used for manual welding only one controller output is adjustable and that is the machine terminal voltage. Thus, the MIMO approach of Abdelrahman (1998), Moore et al. (1999), Naidu et al. (2003) and Jalili-Kharaajoo et al. (2003) is in general not suitable for the manual welding process, which is of concern in this paper. The arc length dynamics can be characterised as a non-linear system, and therefore, a non-linear control strategy is proposed in this paper. The proposed non-linear controller is based on feedback linearisation, which has the advantage that linear system

theory can be applied when considering stabilisation and performance. This method was also presented in a recent paper (Thomsen, 2005a), but the paper only addressed spray GMAW and the pulsed GMAW was not considered.

Metal transfer control refers to the task of providing detachment of liquid metal drops from the tip of the welding electrode, and in pulsed GMAW this is done by forcing current pulses onto the process. In general it is desirable to have One Drop Per Pulse (ODPP), and also, in many applications a low-pulse energy is preferred. ODPP can be regarded as a robustness property, and thus, ODPP should be fulfilled despite disturbances in the process. Traditionally, pulsed GMAW is carried out by a metal transfer controller, which uses a fixed pulse shape and a fixed pulse frequency. However, using this control method, the pulses need to be oversized (in terms of magnitude and duration) to ensure drop detachment in the presence of disturbances. In this paper, a metal transfer controller, which can handle disturbances without using oversized pulses, is proposed. The basic aim is to obtain a uniform drop size prior to pulse initiation by integrating the melting speed. The proposed metal transfer controller is also explained by Thomsen (2005b) and is a continuation of the work by Thomsen (2004). Other work in the area of pulsed GMAW typically involves tuning pulse parameters in the traditional control scheme. Also, work has been done on pulse shapes, for example, the double pulse approach by Zhang and Li (2001).

The primary objective in this paper is to give a full overview of the pulsed GMAW process and evolve a novel high-performance control strategy for the whole welding system and process.

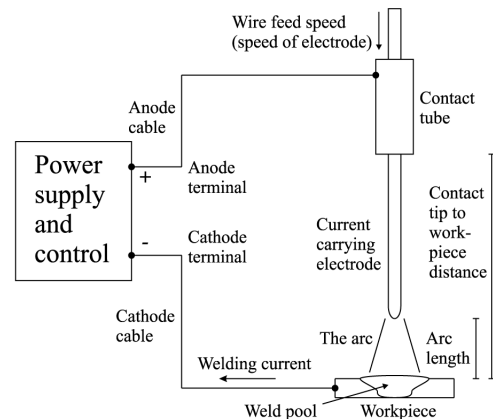
## 2 Gas metal arc welding

In the following, the pulsed GMAW process is described and a mathematical model of the process is presented. Also, the related hardware is described and an overview of the control system is given.

### 2.1 The GMAW process

The GMAW process is illustrated in Figure 1. The welding machine outputs a voltage at the terminals, which powers an electrical circuit consisting of the anode cable, the cathode cable, the electrode and the arc. The energy produced in the arc and the electrode melts the electrode and causes drop growth and drop detachment from the tip of the electrode. The electrode, consumed, is replaced by a new electrode and is supplied by a wire feed system. Energy generated in the arc also melts the workpiece and melted workpiece material and detached liquid metal drops from the electrode form a weld pool. When the weld pool cools down and solidifies, the weld is complete. During the welding process, the arc is protected from the ambient air using some shielding gas, typically, pure argon or a mixed gas of argon and carbon dioxide.

**Figure 1** Illustration of the GMAW process. A consumable electrode is fed by a wire feed system (not shown) through the contact tube (tip). The electrode melts and liquid metal drops detach and fall into the weld pool



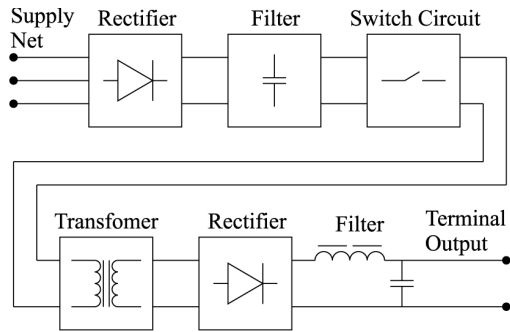
GMAW can be divided into at least three modes of operation depending on the current. These modes are the short arc mode the globular mode and the spray mode. In the short arc mode, the tip of the electrode with the pendant drop is periodically short circuited with the workpiece, causing a sudden increase in current and thereby a release of energy, which detaches the drop. Typically, the short arc mode can be used up to an average current of around 200 A depending on the electrode material and diameter. In the spray mode, the electrode is ideally never short circuited with the workpiece. In the spray mode the current is stronger, typically, a minimum of 250 A, and because of the strong current, drops are detached from the electrode without touching the workpiece. The globular mode refers to the region, with respect to current, between the short arc mode and the spray mode. In this mode the size of the drops detaching from the electrode is in general larger and more irregular compared to the drops in the spray mode. The globular mode produces a poor weld, and thus, this mode is normally avoided. In ordinary spray welding, a strong current is maintained during the welding process. However, a similar drop detachment behaviour can be obtained by shifting the current between a high and a low level. This is referred to as pulsed GMAW. During the time intervals with a low current level, also denoted as the base periods, the arc is maintained but ideally no drop detachments occur. During the time intervals with a high current level, also denoted as the pulse periods, drops are detached from the electrode. Ideally, one drop should be detached for every pulse period. In this paper, the focus especially is on control of the pulsed GMAW process, though, ordinary spray welding can also be included in the framework.

### 2.2 System overview

Traditionally, welding machines were built on transformer technology, such that, a high voltage and a weak current are transformed into a low voltage and strong current. Also, a large choke was included in the machine to maintain the arc during welding and to provide the desired dynamic characteristics. In modern welding machines

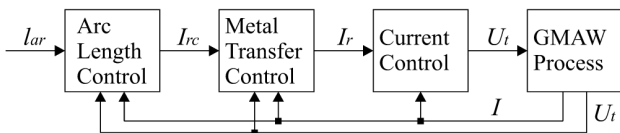
the voltage and current, likewise is transformed but rather through a switched voltage converter. Basically, the net supply voltage is rectified into a DC voltage and then the voltage is converted by a switching circuit and a transformer into a controlled and lower output voltage. Ideally, the transformer has no influence on the dynamics of the process. Afterwards, the voltage is evened by some hardware filter. As an example the power supply part of a Migatron Flex 4000 welding machine is shown in Figure 2 (see Thomsen, 2004).

**Figure 2** Main components of the power supply part of a Migatron Flex 4000 welding machine



The switched circuit in the power supply is essentially controlled by the algorithm controlling the welding process. A general framework of a controller for the pulsed GMAW process is illustrated in Figure 3 where it is assumed that it is only possible to measure the machine terminal voltage  $U_t$  and the current  $I$ . These measurements can be considered as the standard available measurements in manual welding. The output from the welding machine is the control voltage, which ideally is equal to the machine terminal voltage  $U_t$ .

**Figure 3** The cascade coupled control system for the manual pulsed GMAW process

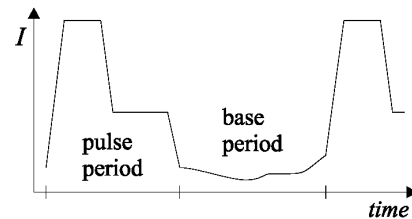


Two main tasks can be identified for control of the pulsed GMAW process. These tasks are arc length control and metal transfer control, which can be configured in the cascade coupled control structure shown in Figure 3. As previously described, control of the GMAW process can be divided into base periods and pulse periods. Normally, arc length control is performed in the base period while metal transfer control is performed in the pulse period.

The main objective in arc length control is to keep a steady arc length in spite of disturbances such as unevenness in the workpiece and uneven movement of the welding gun. Arc length control is performed by adjusting the current reference control signal  $I_{rc}$  to keep the arc length  $l_a$  at the arc length reference  $l_{ar}$ . As arc length control is performed during the base period, the control signal  $I_{rc}$  is simply connected to the current reference signal  $I_r$  during this period. The objective in metal transfer control is basically to provide drop detachment from the electrode.

This is done during the pulse period by forcing a current pulse onto the process by shaping the current reference signal  $I_r$ . Therefore, in the pulse period the control signal  $I_{rc}$  from the arc length controller is disregarded. By inserting a current controller in the welding machine, the welding current is determined by this control loop, and thus, the welding machine acts as a controlled current source. Such internal current controller provides a direct way to shape current pulses and handle extreme situations such as short circuits, which might otherwise damage the machine. It is believed that such current controller is normally included in modern welding machines, and likewise it is included in the present control system. In Figure 4, a typical current shape generated by modern welding machines is shown. In the base period the current is shaped by the arc length controller and the current control loop keeps the current close to the set point. Similarly, the current is shaped by the metal transfer controller during the pulse period. Normally, in modern welding machines, the length of the base periods and the pulse periods are fixed, and thus, the pulse frequency is also fixed. Such a scheme can be denoted as a Fixed Frequency Metal Transfer Controller (FFMTC).

**Figure 4** Sketch of the current during the pulse period and base period



### 2.3 Dynamical model

For control a suitable model of the welding process is needed. Such a model can be found in numerous works, for example, by Naidu et al. (2003) or Thomsen (2004). The main parts of the model will be presented as follows. Basically, the important aspects with respect to control are the electrical circuit, the drop dynamics, the drop detachment criteria and the melting rate.

The GMAW process constitutes an electrical circuit, which can be described by Equation (1).  $U_t$  is the machine terminal voltage,  $R_w$  is the cable resistance,  $L_w$  is the cable inductance,  $l_s$  is the electrode length,  $\rho_r$  is the electrode resistivity and  $I$  is the welding current.

$$U_t = R_w I + L_w \dot{I} + l_s \rho_r I + U_a \quad (1)$$

$U_a$  is the arc voltage, which can be modelled as in Equation (2), see, for example, Naidu et al. (2003).  $U_0$  is a constant voltage potential,  $R_a$  is the arc resistance and  $E_a$  is a constant describing the relationship between arc length and voltage

$$U_a = U_0 + R_a I + E_a l_a \quad (2)$$

Equation (1) describes the current dynamics in the GMAW process. However, as described in the previous section, in general welding machines are equipped with an inner current control loop that determines the current dynamics.

The inner closed loop dynamics can be approximated by a first-order system as in Equation (3) (see Thomsen, 2004).  $\tau_i$  is the time constant for the system and  $I_r$  is input, that is, the current reference:

$$\dot{I} = -\frac{1}{\tau_i}I + \frac{1}{\tau_i}I_r \quad (3)$$

The pendant drop attached to the tip of the electrode can be modelled as a mass-spring-damper system as described by Watkins et al. (1992), Choi et al. (2001) and Wu et al. (2004). The mass-spring-damper system is given by Equation (4), where  $m_d$  is the mass of the drop,  $x_d$  is the position of the drop (with respect to the electrode),  $b_d$  is the damping coefficient,  $k_d$  is the spring constant and  $F_T$  is the sum of other forces:

$$m_d \ddot{x}_d = F_T - b_d \dot{x}_d - k_d x_d \quad (4)$$

$F_T$  is stated in Equation (5) and consists of a gravity force  $F_g$ , an electromagnetic force  $F_{em}$ , an aerodynamic drag force  $F_d$  and a momentum force  $F_m$  accounting for the change of mass of the drop:

$$F_T = F_g + F_{em} + F_d + F_m \quad (5)$$

The electromagnetic force  $F_{em}$  will dominate the other forces with strong currents. Strong current is present in the pulse periods and therefore the electromagnetic force, which is described by Equation (6), is important with respect to metal transfer control. A derivation of the electromagnetic force can be found by Amson (1965) and Lancaster (1986) and also see Jones et al. (1998) for the significance of the electromagnetic force in pulsed welding.  $\mu_0$  is the permeability of free space,  $r_d$  is the radius of the drop,  $r_e$  is the radius of the electrode and  $\theta$  an angle representing the area of the conducting area of the drop.

$$F_{em} = \frac{\mu_0 I^2}{4\pi} \left[ \ln \left( \frac{r_d \sin \theta}{r_e} \right) - \frac{1}{4} - \frac{1}{1 - \cos \theta} + \frac{2}{(1 - \cos \theta)^2} \ln \left( \frac{2}{1 + \cos \theta} \right) \right] \quad (6)$$

In the literature prediction of drop detachments is either described by the Static Force Balance Model (SFBM), that has been extended to a Dynamic Force Balance Model (DFBM) or described by a model based on the Pinch Instability Theory (PIT). The SFBM drop detachment criterion is stated in Equation (7), and it predicts drop detachment by comparing the surface tension force  $F_s$  of the drop with the external forces  $F_T$  exerted on the drop (see Watkins et al., 1992).  $r_e$  is the radius of the electrode and  $\gamma_{st}$  is the surface tension.

$$\text{SFBM detachment if: } F_T > F_s = 2\pi r_e \gamma_{st} \quad (7)$$

In the SFBM, the dynamics of the drop is not taken into account when predicting the occurrence of drop detachment. However, in Choi et al. (2001) dynamics are accounted for by including the inertia of the drop in the model. This gives the DFBM as stated in Equation (8).

$$\text{DFBM detachment if: } F_T + m_d \ddot{x}_d > F_s = 2\pi r_e \gamma_{st} \quad (8)$$

The drop detachment criteria given by SFBM and DFBM rely on the axial forces acting on the drop. However, the drop detachment criterion based on the PIT relies on the radial forces acting on the drop. The PIT criterion states that drop detachment occurs if the drop radius  $r_d$  exceeds a critical drop radius  $r_{dc}$ . The PIT criterion (see Lancaster, 1986) is stated in Equation (9), where  $\mu_0$  is the permeability of free space and  $\rho_e$  is the density of the electrode material.

PIT detachment if:  $r_d > r_{dc}$

$$r_{dc} = \frac{\pi(r_d + r_e)}{\frac{5}{4} \left( \frac{x_d + r_d}{r_d} \right) \left( 1 + \frac{\mu_0 I^2}{2\pi\gamma(r_d + r_e)} \right)^{0.5}}, \quad r_d = \left( \frac{3m_d}{4\pi\rho_e} \right) \quad (9)$$

The melting speed can be modelled in two ways: that is, the anode heating and the Ohmic heating (see Lesnewich, 1958). The anode heating represents the kinetic energy of electrons bombarding the electrode, and also, the energy of condensation when electrons are absorbed into the lattice of the electrode material. Ohmic heating is caused by the energy loss from the current flowing through the electrode material. The melting speed model is stated in Equation (10) where  $k_1$  and  $k_2$  are constants used for the anode heating and the Ohmic heating, respectively:

$$v_m = k_1 I + k_2 I^2 \quad (10)$$

In Table 1, the units and values of the parameters used in this section are shown. In Sections 3.3 and 4.2, these parameters are used for numerical simulation. Moreover, in Table 2, the variables used in the model are given.

**Table 1** Model parameters

Symbol	Unit	Value	Description
$R_w$	$\Omega$	0.004	Cable resistance
$L_w$	H	$15 \times 10^{-6}$	Cable inductance
$\rho_r$	$\Omega/\text{m}$	0.2821	Electrode resistivity (steel)
$r_e$	m	$5 \times 10^{-4}$	Electrode radius
$U_0$	V	15.7	Arc voltage constant
$R_a$	$\Omega$	0.022	Arc resistance
$E_a$	V/m	636	Arc length factor
$\tau_i$	s	$6.7 \times 10^{-6}$	Time constant
$K_1$	m/(s A)	$3.7 \times 10^{-4}$	Melting speed constant
$K_2$	1/(A <sup>2</sup> m)	$6.6 \times 10^{-4}$	Melting speed constant
$v_e$	m/s	0.267	Wire feed speed
$b_d$	kg/s	0.0008	Drop damping constant
$k_d$	N/m	3.5	Drop spring constant
$\mu_0$	(kg m)/(A <sup>2</sup> s <sup>2</sup> )	$1.257 \times 10^{-6}$	Permeability of free space
$\theta$	rad	$0.5\pi$	Conducting area
$\gamma_{st}$	N/m <sup>2</sup>	2	Steel surface tension

**Table 2** Model variables

Symbol	Description
$l_a$	Arc length
$I$	Current
$U_t$	Terminal voltage
$l_s$	Electrode stick-out
$m_d$	Mass of drop
$x_d$	Drop extension
$F_T$	Total axial force
$F_g$	Gravity force
$F_{em}$	Electromagnetic force
$F_d$	Drag force
$F_m$	Momentum force
$F_s$	Surface tension force
$r_d$	Drop radius
$r_{dc}$	Critical drop radius
$v_m$	Melting speed
$l_c$	Contact tip to workpiece distance

### 3 ARC length control

As described in the previous section arc length control is one of the main tasks in GMAW. The arc length is determined by the melting speed  $v_m$ , the wire feed speed  $v_e$  and disturbances in the contact tip to workpiece distance  $l_c$ . From Equation (10), it can be seen that the melting speed depends on the current dynamics, which is described by Equation (3). If disturbances are neglected a nominal model describing the arc length dynamics can be derived:

$$\dot{l}_a = v_m - v_e = k_1 I + k_2 I^2 (l_c - l_a) - v_e \quad (11)$$

Let us use Equations (3) and (11) for setting up a state space description of the arc length process. Let  $x$  be a vector containing two states  $x_1$  and  $x_2$ , where  $x_1 = I$  and  $x_2 = l_a$ . Moreover,  $u = I_r$  is the input and  $y = l_a$  is the output. Now, the non-linear dynamic system can be formulated:

$$\dot{x} = f(x) + g(x)u \quad (12)$$

$$y = h(x) \quad (13)$$

where

$$f(x) = \begin{bmatrix} f_1(x) \\ f_2(x) \end{bmatrix} = \begin{bmatrix} -x_1 / \tau_i \\ k_1 x_1 + k_2 x_1^2 (l_c - x_2) - v_e \end{bmatrix} \quad (14)$$

$$g(x) = \begin{bmatrix} g_1(x) \\ g_2(x) \end{bmatrix} = \begin{bmatrix} 1 / \tau_i \\ 0 \end{bmatrix} \quad (15)$$

$$h(x) = x_2 \quad (16)$$

This model is used for developing an arc length controller. A non-linear controller based on feedback linearisation is developed. Such controller has the advantage that, non-linearities can be accounted for, and also, in operating points need to be selected and therefore only one controller has to be tuned. Moreover, the feedback linearisation approach has the advantage that it is possible to tune the system using standard linear techniques.

### 3.1 Feedback linearisation

The idea in feedback linearisation is to use a transformation  $z = T(x)$  and apply some feedback control law  $u$  that transforms the non-linear system into a linear system (see Khalil, 2002). Then, having obtained a linear system ordinary linear control design methods can be applied for stabilisation and performance. Given the non-linear system in Equations (12) and (13), the goal is to find some transformation  $z = T(x)$  that transforms the system into the system stated in Equations (17) and (18).

$$\dot{z} = A_c z + B_c \gamma(x) [u - \alpha(x)] \quad (17)$$

$$y = C_c z \quad (18)$$

The terms  $\gamma(x)$  and  $\alpha(x)$  are functions of the original states  $x$ . The matrices  $A_c$ ,  $B_c$  and  $C_c$  are on the control canonical form stated in Equation (19).

$$A_c = \begin{bmatrix} 0 & 1 \\ 0 & 0 \end{bmatrix}, \quad B_c = \begin{bmatrix} 0 \\ 1 \end{bmatrix}, \quad C_c = [1 \quad 0] \quad (19)$$

Basically, if it is possible to find a transformation that transforms the original non-linear system into a system on the form stated in Equations (17) and (18), then the system feedback is linearisable. This means that the system can be linearised using the control law stated in Equation (20):

$$u = \alpha(x) + \beta(x)v, \quad \beta(x) = \frac{1}{\gamma(x)} \quad (20)$$

Inserting this control law into (Equation (17)) gives a linear system having input  $v$ :

$$\dot{z} = A_c z + B_c v \quad (21)$$

$$y = C_c z \quad (22)$$

In general, it is not trivial (or if possible at all) to find a transformation  $T(x)$  that transforms a non-linear system into the form given in Equations (17) and (18). Also, the non-linear system might be partially feedback linearisable, leaving some internal dynamics. However, for some non-linear systems the system is fully linearisable, and moreover, a transformation can be found using a standard approach (see Khalil, 2002). In fact, this is the case for the dynamic arc length model derived in the previous section.

The relative degree  $\rho$  equals the number of derivatives of  $h(x)$  before dependence on the input  $u$  is obtained. For the dynamic arc length model the relative degree is equal to two, as dependence of  $u$  is obtained for the second derivative of  $h(x)$ . As the system order also equals two the system feedback is fully linearisable. Standard expressions for  $\gamma(x)$  and  $\alpha(x)$  are stated in Equations (23) and (24):

$$\gamma(x) = L_g L_f^{\rho-1} h(x) \quad (23)$$

$$\alpha(x) = -\frac{1}{\gamma(x)} L_f^\rho h(x) \quad (24)$$

$L_f$  and  $L_g$  are Lie derivatives with respect to  $f(x)$  and  $g(x)$ , respectively (see Khalil, 2002). For example,

$L_f h(x) = (\partial h(x)/\partial x)f(x)$ . Using  $\rho = 2$  and Equations (12) and (13) the functions  $\gamma(x)$  and  $\alpha(x)$  can be calculated:

$$\gamma(x) = (k_1 + 2k_2x_1(l_c - x_2))\frac{1}{\tau_i} \quad (25)$$

$$\alpha(x) = -\frac{1}{\gamma(x)}(\gamma(x)\tau_i f_1 - k_2x_2f_2) \quad (26)$$

The transformation  $T(x)$  is given by the output equation  $h(x)$  and its first derivative.

$$z = \begin{bmatrix} z_1 \\ z_2 \end{bmatrix} = \begin{bmatrix} T_1(x) \\ T_2(x) \end{bmatrix} = \begin{bmatrix} h(x) \\ L_f h(x) \end{bmatrix} = \begin{bmatrix} x_2 \\ f_2(x) \end{bmatrix} \quad (27)$$

Now, having found a transformation  $T(x)$  and the functions  $\gamma(x)$  and  $\alpha(x)$  the system stated in Equations (12) and (13) has been transformed into a system having the structure of Equations (17) and (18). In this representation, the first state  $z_1$  is the arc length  $l_a$  and the second state  $z_2$  is the derivative of the arc length, that is,  $dl_a/dt$ .

### 3.2 Non-linear arc length control

The objective is to control the arc length. This means, the arc length controller must be stable and should drive the arc length  $l_a = x_2$  towards the reference arc length  $l_{ar} = r$ .

Now, the idea is to develop a state feedback controller that is able to drive the two states towards some settings. The first state  $z_1$  is the arc length, which must be driven towards some reference  $r$ . The second state  $z_2$  equals the derivative of the first state, and thus,  $z_2$  must be driven towards the derivative of the reference. Therefore, the error dynamics must be considered. Firstly, let us define the error  $e$ :

$$e = R - z, \quad R = [r \quad \dot{r}]^T \quad (28)$$

Now, using Equation (17), describing the system dynamics, the error dynamics can be derived:

$$\dot{e} = A_c e - B_c \gamma(x)[u - \alpha(x)] + B_c \ddot{r} \quad (29)$$

The feedback on error dynamics can be linearised using a control law that cancels the non-linear terms, and then leaves a linear part that can be stabilised by the state feedback  $K_c e$  where  $K_c = [k_{c1} \ k_{c2}]$ :

$$u = \alpha(x) + \beta(x)[K_c e + \ddot{r}], \quad \beta(x) = \frac{1}{\gamma(x)} \quad (30)$$

If the control law, stated in Equation (30), is inserted into the error dynamics the following result is obtained:

$$\dot{e} = (A_c - B_c K_c) e \quad (31)$$

Hence, using Equation (30) for the control law the error dynamics becomes linear, and moreover, the error dynamics is stable if the matrix  $(A_c - B_c K_c)$  is stable (Hurwitz). Thus, ensuring stability, and also performance, is a matter of choosing  $K_c$ .

However, disturbances and uncertainties might result in a steady state offset in the arc length. For some disturbances and uncertainties an offset can be removed by

including integral control in the control law. Therefore, let us introduce a variable  $\sigma$ , which is the integral of the arc length error  $e_1$ . This dynamics can be added to the dynamics describing the arc length process to obtain an augmented system. Let us define a new state vector  $\psi = [e_1, e_2, \sigma]^T$ . Now, the augmented system is given by:

$$u = \alpha(x) + \beta(x)\psi, \quad \beta(x) = \frac{1}{\gamma(x)} \quad (32)$$

where

$$A_c = \begin{bmatrix} 0 & 1 & 0 \\ 0 & 0 & 0 \\ 1 & 0 & 0 \end{bmatrix}, \quad B_c = \begin{bmatrix} 0 \\ 1 \\ 0 \end{bmatrix}, \quad C_c = [1 \ 0 \ 0] \quad (33)$$

Again, a control law can be found which linearises the system, and now  $K_a = [k_{a1} \ k_{a2} \ k_{a3}]$ .

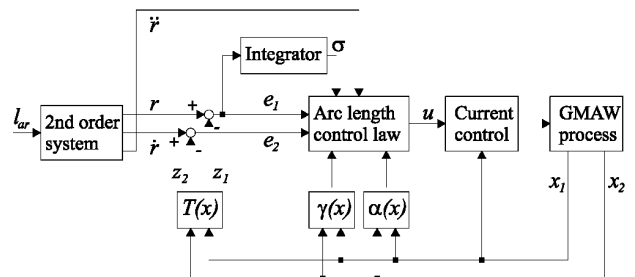
$$u = \alpha(x) + \beta(x)[K_a \psi + \ddot{r}], \quad \beta(x) = \frac{1}{\gamma(x)} \quad (34)$$

Now, the following closed loop dynamics is obtained.

$$\dot{\psi} = (A_c - B_c K_a) \psi \quad (35)$$

Hence, using Equation (34) for the control law the  $\psi$  dynamics becomes linear, and moreover, the  $\psi$  dynamics is stable if the matrix  $(A_c - B_c K_a)$  is stable. As before, ensuring stability and performance is a matter of choosing  $K_a$ . For instance, the feedback vector  $K_a$  can be obtained from a pole placement approach, in which, the closed loop is shaped to some prototype design (see Franklin et al., 1994). Here, the closed loop dynamics is shaped as a Bessel filter. For purpose of simulation in Section 3.3 the following feedback vector is used:  $K_a = [6.23 \times 10^5; 1.22 \times 10^3; 1.27 \times 10^8]$ . In Figure 5, the arc length control system is sketched.

**Figure 5** The control structure. The second order system generates the reference signals.  $\gamma(x)$  and  $\alpha(x)$  feedback linearises the system and  $T(x)$  transforms the original process states into the  $z$  states



From Equation (34), we see that both the reference  $r$ , the first derivative of  $r$  and the second derivative of  $r$  are needed. As shown in Figure 5, these signals are provided from a second order system filtering the original reference signal  $l_{ar}$ .

The control law in Equation (34) is a state feedback control law. Thus, it is assumed that the states  $\psi_1 = e_1 = r - z_1$  and  $\psi_2 = e_2 = dr/dt - z_2$  can be measured. Both  $z_1$  and  $z_2$  depend on the states  $x_1$  and  $x_2$ , that is, the current and the arc length. Normally, the current is

measured directly in the system by a current sensor (hall sensor), but only the arc length is indirectly measured. The arc length can be estimated using the arc voltage model in Equation (2). Thus, the current  $I$  and the arc voltage  $U_a$  must be measured to calculate the arc length  $l_a$ . However, in most welding systems the arc voltage is not measured, but instead the voltage  $U_t$  at the welding machine terminals is measured. The terminal voltage  $U_t$  includes voltage drops over the cables, the electrode and the arc. The cable current dynamics is very fast as the cable inductance is rather low, and therefore, a steady state expression for  $U_t$  can be used:

$$U_t = R_1 I + U_a, \quad R_1 = R_w + \rho_r l_{s0} \quad (36)$$

$l_{s0}$  is the expected or average length of the electrode, which is set to 0.005 m. Now, using Equations (2) and (36), an arc length estimate,  $\hat{x}_2 = \hat{l}_a = \hat{z}_1$ , can be found:

$$\hat{l}_a = \hat{x}_2 = \hat{z}_1 = \frac{U_t - R_1 I - U_0 - R_a I}{E_a} \quad (37)$$

Hence, the estimate  $\hat{x}_2$  or  $\hat{z}_1$  in Equation (37) is used instead of  $x_2$  or  $z_1$  in Equation (34).

### 3.3 Model uncertainty

The feedback linearisation controller described in the previous section uses a model of the real process to cancel non-linear terms. However, this model is not exact and therefore robustness should be addressed. Here, robustness of the closed loop system is investigated by simulation.

Figure 6 shows a simulation of the nominal arc length system Equations (12) and (13) with disturbances in the contact tip to workpiece distance  $l_c$ . In Figure 6, the current  $I$ , the arc length  $l_a$  and the contact tip to workpiece distance  $l_c$  are shown, which has a nominal value of 0.015 m. The reference arc length is set to 3 mm, and 20 Hz bandlimited noise is applied to  $l_c$  to simulate disturbances from the hand-held welding gun. Also, at time  $t = 0.5$  s the contact tip to workpiece distance is changed from an average of 15–10 mm. The parameters used for simulation are shown in Table 1, where the melting speed constants are derived from melting rate constants in Moore et al. (1997). Also, values for  $U_0$ ,  $R_a$ ,  $E_a$  and  $\rho_r$  are obtained from Moore et al. (1997). The other parameters are realistic estimates when considering a real welding process. However, it should be noted that precise values are not of concern in this paper, as the values are used only for numerical simulation.

In the control law Equation (34) values for  $\gamma(x)$ ,  $\alpha(x)$ ,  $T_1(x)$  and  $T_2(x)$  must be calculated. These terms depend on uncertain parameters and variables. For example,  $\gamma(x)$  depends on the melting speed coefficients  $k_1$  and  $k_2$ , the contact tip to workpiece distance  $l_c$ , the current time constant  $\tau_r$ , the current measurement, and the estimate of the arc length which again depends on the arc length model. Probably, all of these parameters and variables contain some uncertainty and this results in an overall uncertainty in  $\gamma(x)$ . To investigate uncertainty a number of simulations are performed with perturbed terms  $\gamma(x)$ ,  $\alpha(x)$ ,  $T_1(x)$  and  $T_2(x)$ . In turn, each of the terms is chosen

either larger or smaller than the nominal value, while the other terms are held at the nominal value. In Figures (7) and (8), the arc length for each simulation is shown. The uncertainties used in each simulation are shown in Table 3. In Table 3,  $K_\gamma$ ,  $K_\alpha$ ,  $K_{T_1}$  and  $K_{T_2}$  denotes the multiplicative uncertainty used for each term. For example,  $K_\gamma$  is the multiplicative uncertainty on  $\gamma(x)$ . Moreover, the disturbances in the contact tip to workpiece distance  $l_c$ , shown in Figure 6(c), are included in the simulations.

From Figure 7(a) and (b) it can be seen that despite large perturbations (a factor 5 and a factor 0.2) in  $\gamma(x)$  the closed loop system is stable and the disturbances in  $l_c$  can be handled. However, as it can be seen in Figure 7(c) and (d) perturbations in  $\alpha(x)$  affect the closed loop behaviour much more. In fact, for a relative small positive perturbation in  $\alpha(x)$  (a factor 1.04) the system almost becomes unstable. On the other hand, if  $\alpha(x)$  is lowered to 0.6 times the nominal value the ability to handle disturbances is rather low.

**Figure 6** Simulation of the nominal system: (a) the welding current  $I$ , (b) the arc length  $l_a$  and (c) the contact tip to workpiece distance  $l_c$

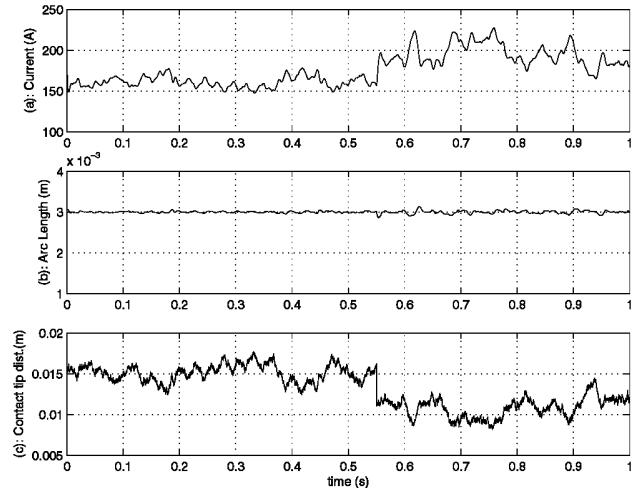


**Figure 7** The arc length for perturbations in  $\gamma(x)$  and  $\alpha(x)$ : (a) positive perturbation in  $\gamma(x)$ , (b) negative perturbation in  $\gamma(x)$ , (c) positive perturbation in  $\alpha(x)$  and (d) negative perturbation in  $\alpha(x)$

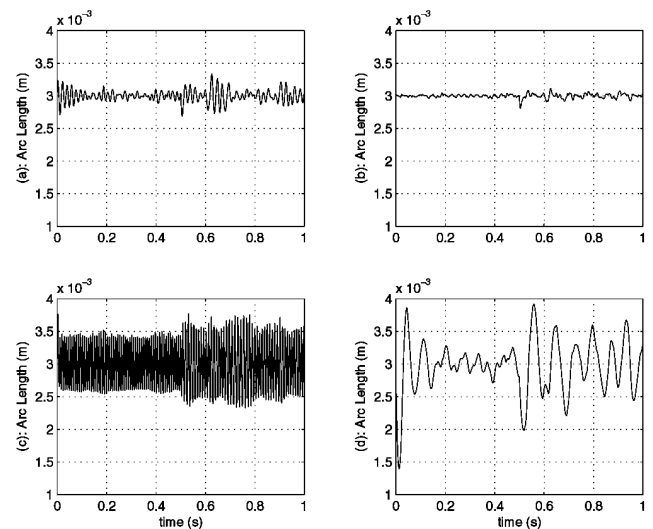


**Figure 8** The arc length for perturbations in  $T_1(x)$  and  $T_2(x)$ : (a) positive perturbation in  $T_1(x)$ , (b) negative perturbation in  $T_1(x)$ , (c) positive perturbation in  $T_2(x)$  and (d) negative perturbation in  $T_2(x)$

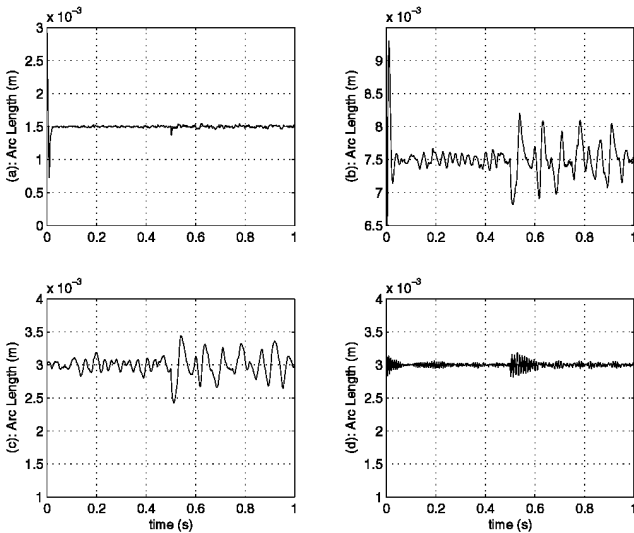


**Table 3** Model uncertainty

Figure	$K_\gamma$	$K_\alpha$	$K_{T1}$	$K_{T2}$
Figure 7(a)	5	1	1	1
Figure 7(b)	0.2	1	1	1
Figure 7(c)	1	1.04	1	1
Figure 7(d)	1	0.6	1	1
Figure 8(a)	1	1	2	1
Figure 8(b)	1	1	0.4	1
Figure 8(c)	1	1	1	5
Figure 8(d)	1	1	1	0.2

From Figure 8(a) and (b) it can be seen that perturbations (a factor 2 and a factor 0.4) in  $T_1(x)$  affects the steady state value of the arc length, but otherwise the closed loop system is stable and disturbances in  $l_c$  can be handled. From Figure 8(c) and (d) it can be seen that even large perturbations (a factor 5 and a factor 0.2) in  $T_2(x)$  can be tolerated, that is, the closed loop system is stable and disturbances can be handled.

From the simulations it can be seen that uncertainties in the four terms affect the stability and behaviour of the closed loop system. However, some uncertainties have a significant effect on the closed loop system, while some uncertainties have a rather insignificant effect. For  $\gamma(x)$  large perturbations can be tolerated, and thus, uncertainty in  $\gamma(x)$  only has a small effect on the closed loop system. Uncertainty in  $\alpha(x)$ , on the other hand, has a significant influence on the closed loop system. If  $\alpha(x)$  is a few percent too large the system becomes unstable, and if  $\alpha(x)$  is too small the system easily becomes rather slow. However,  $\alpha(x)$  does not have to be exact, and it seems that an  $\alpha(x)$  around 60% and up to 100% of the real value could be used. Uncertainty in  $T_1(x)$  and  $T_2(x)$  are less significant than uncertainty in  $\alpha(x)$ . Especially for  $T_2(x)$  large perturbations can be accepted. However, uncertainty in  $T_1(x)$  affects the steady state offset on the arc length. Though, in practice such offset could easily be removed by tuning the parameters in  $T_1(x)$ .

## 4 Metal transfer control

In pulsed GMAW current pulses are used for detaching drops from the tip of the electrode, such that, one drop is detached for every pulse. Lack of drop detachment or multiple drop detachments for each pulse will have a negative effect on the quality of the weld. Thus, an objective in pulsed GMAW control is to obtain ODPP. This can also be regarded as an objective of robustness. Moreover, in many applications it is important to avoid heating up the electrode or the workpieces too much. For example, this could be the case when welding with alloys or when welding in thin materials. In pulsed GMAW most heating is generated in the pulse period, and thus, minimisation of the energy per pulse used for detaching one drop is desirable. Therefore, a second objective in pulsed GMAW control can be defined as minimisation of the energy per pulse used for detaching one drop.

Three models for drop detachment have been presented, that is, the SFBM, the DFBM and the model based on the PIT. In both the SFBM and the DFBM, drop detachment depends on the total force  $F_T$ . Because of the strong pulse current the electromagnetic force  $F_{em}$  is the far most significant force of the forces included in  $F_T$ . From Equation (6), it can be seen that  $F_{em}$  depends on the size of the drop, that is, drop radius  $r_d$ . In DFBM, the drop detachment criterion also depends on the acceleration of the drop, and a large acceleration is caused by large changes in the total force  $F_T$  which is dominated by  $F_{em}$ . Therefore, as  $F_{em}$  depends on the magnitude of the current the DFBM also becomes dependent of the change in current, that is,  $dI/dt$ . However, the acceleration not only depends on the change of force, but again, on the size of the drop, as small drops for some applied force obtain a higher acceleration than large drops. In the detachment model based on the PIT the criterion for drop detachment depends on the drop radius  $r_d$ , on the position of the drop  $x_d$ , and on the magnitude of the current. The position  $x_d$  both depends on the magnitude of the total force, and also it depends on the change in the total force (or change in current), as a sudden change in force gives rise to drop oscillations, and thus, change in  $x_d$ . The conclusion is that no matter which drop detachment criteria is considered drop detachment depends on the drop size. It also appears that the change in current is another important factor. However, in this paper only the drop size is considered.

Now, let us assume that the pulses are given by some fixed shape, such that, all pulses are identical. Also, suppose that because of disturbances the size of the drop immediately before initiation of the pulse period differ from period to period. Then, conventional (over-sized) pulse shapes must be used to ensure drop detachment for all possible drop sizes. For example, if the drop is relatively small, then some specified pulse shape might not be able to detach the drop. So, to ensure drop detachment, also for the small drops, the pulse height or duration must be increased. However, for large drops, the given pulse shape will be over-sized in the sense that the drop is detached in the beginning of the pulse, and thus, the rest of the pulse just contributes to excess melting and a large heat

input into the workpiece. Therefore, in this case the objective of minimal energy for drop detachment is not fulfilled.

Now, it appears that at least two methods for obtaining drop detachments at minimal energy are feasible. One method is to adjust each pulse shape according to the drop size at the beginning of each pulse. Another method is to make sure that the drop size at the commencement of each pulse is constant, and thereby a fixed and minimised pulse shape can be used. In practice, it is difficult to derive the shape of a pulse based on the drop detachment models as these models are not precise, and therefore, it is better to tune a pulse shape from practical experiments. For this reason the latter method is used, that is, to use a fixed pulse shape but ensuring a uniform drop size prior to pulse initiation. So, this uniform drop size approach becomes the basic idea in the metal transfer control algorithm presented in this paper.

#### 4.1 Model based metal transfer control

A control mechanism is required to provide a uniform drop size prior to pulse initiation, and also, in the control mechanism it must be possible to control the arc length. This can be done allowing the arc length controller to operate in the base period, but instead of having a fixed pulse frequency, the length of the base period is adjusted according to the size of the drop. In one full cycle the total melting of electrode consists of the length of melted electrode  $x_{mp}$  in the pulse period and the length of melted electrode  $x_{mb}$  in the base period. These lengths can be expressed by the melting speed  $v_m$ . In each cycle the start of the pulse period is denoted by  $t_0$ , the end of the pulse period is denoted by  $t_1$ , which is also the beginning of the base period, and the end of the base period is denoted by  $t_2$ .

$$x_{mp} = \int_{t_0}^{t_1} v_m(I, l_s) dt \quad (38)$$

$$x_{mb} = \int_{t_1}^{t_2} v_m(I, l_s) dt \quad (39)$$

The total length of melted electrode  $x_{mt}$  is given by

$$x_{mt} = x_{mp} + x_{mb} \quad (40)$$

During welding, the melting speed  $v_m$  can be calculated by using the melting speed model stated in Equation (10). The current  $I$  and the stick-out  $l_s$  are needed to calculate the melting speed, but only the current is measured. To overcome this problem  $l_s$  is simply assumed to be the nominal value.

Each drop starts growing from the point of the previous detachment, and continue to grow until detachment occurs again. Normally, drop detachment takes place during the following pulse period, and therefore, a drop begins and ends in a pulse period. To ensure a uniform drop size prior to pulse initiation the melting speed must be integrated from detachment of the previous drop, but in practice it is difficult to calculate the exact point of drop detachment during the pulse period. However, unless a significant disturbance is applied to the process it can be expected that the drop detaches at

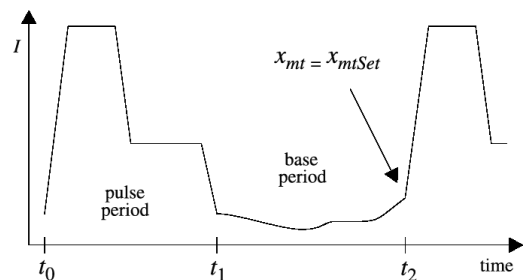
approximately at the same point during each pulse period. This makes it possible to integrate the whole pulse period, and thus, a condition for pulse initiation can be derived. The condition is given in Equation (41) and states that the new pulse period must be initiated when some specified length of electrode  $x_{mtSet}$  has been melted during the pulse and base period. Moreover, to increase robustness of the method a minimal cycle time  $T_{cMin}$  is used as an additional condition in Equation (41).  $t_c$  is the cycle time.

Initiate pulse if:

$$x_{mt} \geq x_{mtSet} \wedge x_{mtSet} \geq T_{cMin} \quad (41)$$

Now, with this condition a uniform drop size prior to pulse initiation is provided. Let us denote this metal transfer controller as the Uniform Drop Metal Transfer Controller (UDMTC). An example pulse and base period are sketched in Figure 9, where the melting speed is integrated from  $t_0$  and until condition Equation (41) is fulfilled.

**Figure 9** Sketch of the current during the pulse period and base period. New pulse initiated at  $t_2$

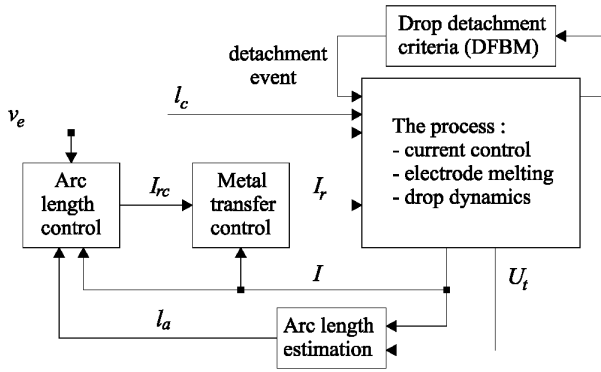


The pulse shape illustrated in Figure 9 is the so-called chair form, which is used in several modern welding machines. Other pulse shapes could likewise be used as for example, the double pulse suggested by Zhang and Li (2001).

#### 4.2 Metal transfer control simulations

In Thomsen (2004), an extensive simulation system for GMAW was presented. This simulation system (developed in Simulink) will be used for validation of the metal transfer control approach described in the previous section. Other works on simulation includes Wang et al. (2004) and Wang et al. (2003). Basically, the simulation system used in this paper is an implementation of the model described in Section 2.3. The simulation system is sketched in Figure 10. The arc length  $l_a$  is measured by an arc length estimator and controlled by the arc length controller. The metal transfer controller applies a reference current  $I_r$  to the process. Other inputs to the process are the wire feed speed  $v_w$ , the contact tip to workpiece distance  $l_c$ , and drop detachment events, which reset the states of the process. The current dynamics is considered to be a part of the welding process and is simply approximated by a first order filter having a time constant  $\tau$ . The process also consists of equations describing electrode melting and drop dynamics. The DFBM criterion is used for determining drop detachment events.

**Figure 10** Simulation system used for investigation of the metal transfer control approach



To enable numerical simulation many parameters are needed. Some parameters are shown in Table 1, though, the wire feed speed is set to 0.1 m/s. A complete list of all parameters and values can be found by Thomsen (2004).

To illustrate the robustness of the proposed metal transfer controller plots from four simulations are shown with comparison to the normal modern approach, namely the FFMTC. In the first simulation the FFMTC is used and in the second simulation the UDMTC is used. In both the first and the second simulation no disturbances are applied to the process. In the third and fourth simulation the FFMTC and the UDMTC are used again, but this time disturbances in the contact tip to workpiece distance are included.

For comparing the two controllers the same pulse shape is used, and also, the FFMTC is adjusted to have the same average frequency as the UDMTC in the simulations without disturbances. Moreover, in the no disturbance situation the fixed pulse shape (which is used in both methods) is tuned to a minimum, such that, no or only a few pulse periods lack drop detachment. In this way the minimal energy objective is fulfilled, but on the other hand the robustness (ODPP) objective is not necessarily obtained.

In Figure 11, the results from the first and the second simulation are shown. The current using the FFMTC is shown in Figure 11(a), the current using the UDMTC is shown in Figure 11(b), and the contact tip to workpiece distance  $l_c$  is shown in Figure 11(c). Drop detachments are indicated by stars on the current plots. As it can be seen there is one pulse in (a) without drop detachment. This might seem odd as  $l_c$  is constant, but the reason is the irregularity of drop oscillations. Thus, the FFMTC is already showing lack of robustness.

In Figure 12, the results from the third and the fourth simulation is shown. As in Figure 11 the currents and drop detachments for FFMTC and UDMTC are shown, and also, the contact tip to workpiece distance  $l_c$  is shown.  $l_c$  is generated by 20 Hz bandlimited noise around the nominal value to simulate irregular movements of the welding gun in manual welding. Furthermore, a positive step equal to 0.003 m at 0.2 s and a negative step of 0.004 m at 0.3 s are included. These steps simulate edges in the workpiece. With these disturbances applied the FFMTC has five pulses without drop detachment and the UDMTC has one pulse without drop detachment. Thus, the UDMTC is far more robust than the FFMTC.

In Figure 13, it can be seen why the UDMTC is more robust than the FFMTC. In (a) the cycle time  $t_c$  is shown for the FFMTC, and the maximal  $t_c$  is fixed as it should be. However, in (b) the cycle time is adjusted according to the UDMTC. The problem for the FFMTC occurs when it is trying to detach a small drop. The UDMTC, on the other hand, waits until the drop is big enough and then initiates the pulse period. Notice that, for robustness the minimal total cycle time  $T_{cMin}$  (see Equation (41)) is set to be a little less than the fixed frequency of the FFMTC.

**Figure 11** (a) Current and drop detachments using the FFMTC, (b) current and drop detachments using the UDMTC. Stars indicates drop detachments and (c) contact tip to workpiece distance

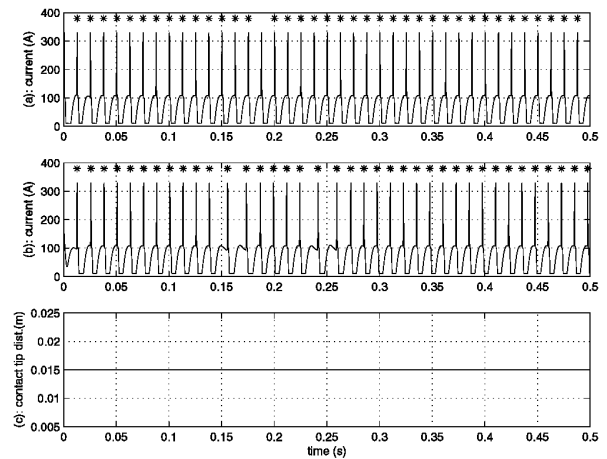


**Figure 12** (a) Current and drop detachments using the FFMTC, (b) current and drop detachments using the UDMTC. Stars indicates drop detachments and (c) contact tip to workpiece distance

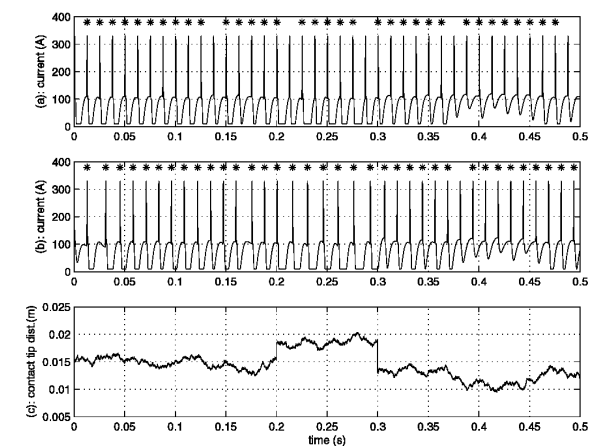
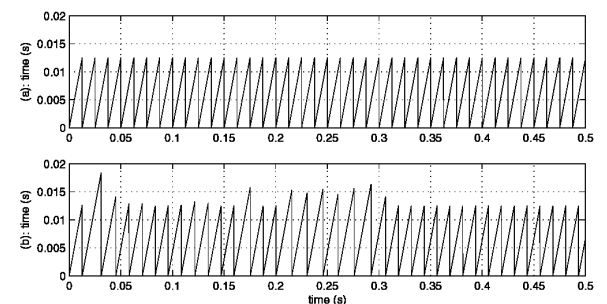


**Figure 13** Cycle time using: (a) the FFMTC and (b) the UDMTC



## 5 Conclusions

In this paper, a controller for the manual pulsed GMAW process has been presented. The control system consists of a current controller, a metal transfer controller and an arc length controller. This can be considered as the normal framework for control of the pulsed GMAW process. However, in this paper, new controllers have been suggested for both arc length control and metal transfer control.

For arc length control a non-linear controller has been described. The controller is based on a non-linear SISO model of the arc length process and uses feedback linearisation for cancellation of non-linear terms. This method has the advantage that traditional linear techniques can be used for tuning the controller. Also, no operating points need to be selected, and therefore, only one linear controller needs to be tuned for all arc length settings and wire feed speed settings. The feedback linearisation method is based on an exact model of the process. However, it cannot be expected that such model is available, and therefore, robustness of the closed loop system is investigated by simulation. This is done by testing the effect of different uncertainties in a simulation environment. The simulation approach does not provide a precise robustness analysis, but rather, it provides information of practical value for the system designer.

For metal transfer control two important objectives are described, that is, ODPP and minimal energy for drop detachment. In this paper a metal transfer controller is proposed which can handle these objectives. The controller is based on obtaining some specified drop size before initiation of each pulse period, and thus the pulse frequency is not fixed. The advantage is an increased robustness towards ODPP objective. Also, it is possible to lower the energy used for drop detachment. The arc length controller and the metal transfer controller have only been tested in simulation. Thus, tests on the real welding process still need to be carried out for both controllers.

## References

- Abdelrahman, M. (1998) 'Feedback linearization control of current and arc length in GMAW system', *Proceedings of the American Control Conference*, Vol. 3, Philadelphia, PA, pp.1757–1761.
- Amson, J. (1965) 'Lorentz force in the molten tip of an arc electrode', *British Journal of Applied Physics*, Vol. 16, pp.1169–1179.
- Choi, J., Lee, J. and Yoo, C. (2001) 'Dynamic force balance model for metal transfer analysis in arc welding', *Journal of Physics D: Applied Physics*, Vol. 34, pp.2658–2664.
- Franklin, G., Powell, J. and Emami-Naeini, A. (1994) *Feedback Control of Dynamic Systems*, 3rd edition, Addison-Wesley.
- Jalili-Kharaajoo, H., Gholampour, V., Ebrahimirad, H. and Ashari, A. (2003) 'Robust nonlinear control of current and arc length in GMAW systems', *Conference on Control Applications*, Vol. 2, pp.1313–1316.
- Jones, L., Eagar, T. and Lang, J. (1998) 'A dynamic model of drops detaching from a gas metal arc welding electrode', *Journal of Physics D: Applied Physics*, Vol. 31, pp.107–123.
- Khalil, H.K. (2002) *Nonlinear Systems*, 3rd edition, Prentice Hall.
- Lancaster, J. (1986) *The Physics of Welding*, Oxford: Pergamon Press.
- Lesnewich, A. (1958) 'Control of the melting rate and metal transfer in gas shielded metal arc welding, part I', *Welding Journal*, pp.343s–353s.
- Moore, K., Abdelrahman, M. and Naidu, D. (1999) 'Gas metal arc welding control – II. control strategy', *Nonlinear Analysis*, Vol. 35, No. 1, pp.85–93.
- Moore, K., Naidu, D., Yender, R. and Tyler, J. (1997) 'Gas metal arc welding control: part 1. modeling and analysis', *Nonlinear Analysis*, Vol. 30, No. 5, pp.3101–3111.
- Naidu, D., Ozcelik, S. and Moore, K. (2003) *Modeling, Sensing and Control of Gas Metal Arc Welding*, Elsevier.
- Ozcelik, S., Moore, K., Naidu, S. and Tyler, J. (1998) 'Classical control of gas metal arc welding', *Trends in Welding Research: Proceedings of the Fifth International Conference*, Pine Mountain, ASM, pp.1033–1038.
- Thomsen, J. (2004) *Advanced Control Methods for Optimization of Arc Welding*, PhD Thesis, Aalborg University, Aalborg, Denmark.
- Thomsen, J. (2005a) 'Feedback linearization based arc length control for gas metal arc welding', *Proceedings of the American Control Conference*, Portland, Oregon, pp.3568–3573.
- Thomsen, J. (2005b) 'Model based metal transfer control', *Seventh International Conference on Trends in Welding Research*, Pine Mountain, ASM.
- Wang, G., Huang, G. and Zhang, Y. (2003) 'Numerical analysis of metal transfer in GMAW', *Metallurgical and Materials Transactions B*, Vol. 34B, No. 3, pp.345–353.
- Wang, G., Huang, G. and Zhang, Y. (2004) 'Numerical analysis of metal transfer in gas metal arc welding under modified pulsed current conditions', *Metallurgical and Materials Transactions B*, Vol. 35B, No. 5, pp.991–999.
- Watkins, A., Smartt, H. and Johnson, J. (1992) 'A dynamic model of droplet growth and detachment in GMAW', *Third International Conference on Trends in Welding Research*, Gatlinburg, ASM, pp.993–997.
- Wu, C., Chen, M. and Li, S.K. (2004) 'Analysis of droplet oscillation and detachment in active control of metal transfer', *Computational Materials Science*, Vol. 31, pp.147–154.
- Zhang, Y. and Li, P. (2001) 'Modified active metal transfer control and pulsed GMAW of titanium', *Welding Journal*, Vol. 80, No. 2, pp.54s–61s.
- Zhang, Y., Liguó, E. and Walcott, B. (2002) 'Robust control of pulsed gas metal arc welding', *ASME Journal of Dynamic Systems, Measurement, and Control*, Vol. 124, No. 2, pp.281–289.